Supplementary Information for:

Incoherent inputs enhance robustness of biological oscillators

Zhengda Li[1,2], Qiong Yang[1,2,†]

[1]Department of Biophysics

[2]Department of Computational Medicine & Bioinformatics

University of Michigan,

Ann Arbor, MI 48109

[†] E-mail: qiongy@umich.edu

Table S1. Parameter ranges in random parameter search, related to STAR Methods: Generalized models for enzymatic networks.

Parameters	Value Range (logarithmic)	Value Range (linear)
k_{act}, k_{inh}	10^{-3} ~10^{1}	0~10
k_{ij}	10^{-1} ~10^{3}	0~1000
n	10^{0} ~10^{1}	1~10
K	10^{-3} ~10^{1}	0~10

Table S2. Parameter ranges in the cell cycle model, related to STAR Methods: Models for real-world biological oscillators.

	Parameter	Nominal value (Tsai et al., 2014)	Parameter range for random parameter simulations with linear range
0	k_{synth}	1.5	0-10
1	k_{dest}	0.4	0-1
2	r	1	1
3	k_{cdc25}	0.0354	0-1
4	k_{wee1}	0.0354	0-1
5	$p1$	5	0-50
6	$p2$	5	0-50

7	$ec50_{cdc25}$	30 nM	0-200 nM
8	n_{cdc25}	11	1-15
9	$ec50_{wee1}$	35 nM	0-200nM
10	n_{wee1}	3.5	1-10
11	k_{plxon}	1.5	0-10
12	k_{plxoff}	0.15	0-1
13	$ec50_{plx}$	60 nM	0-200 nM
14	n_{plx}	5	2-6
15	k_{apcon}	1.5	0-10
16	k_{apcoff}	0.125	0-1
17	$ec50_{apc}$	0.5	0-1
18	n_{apc}	4	2-6

Supplemental Figures

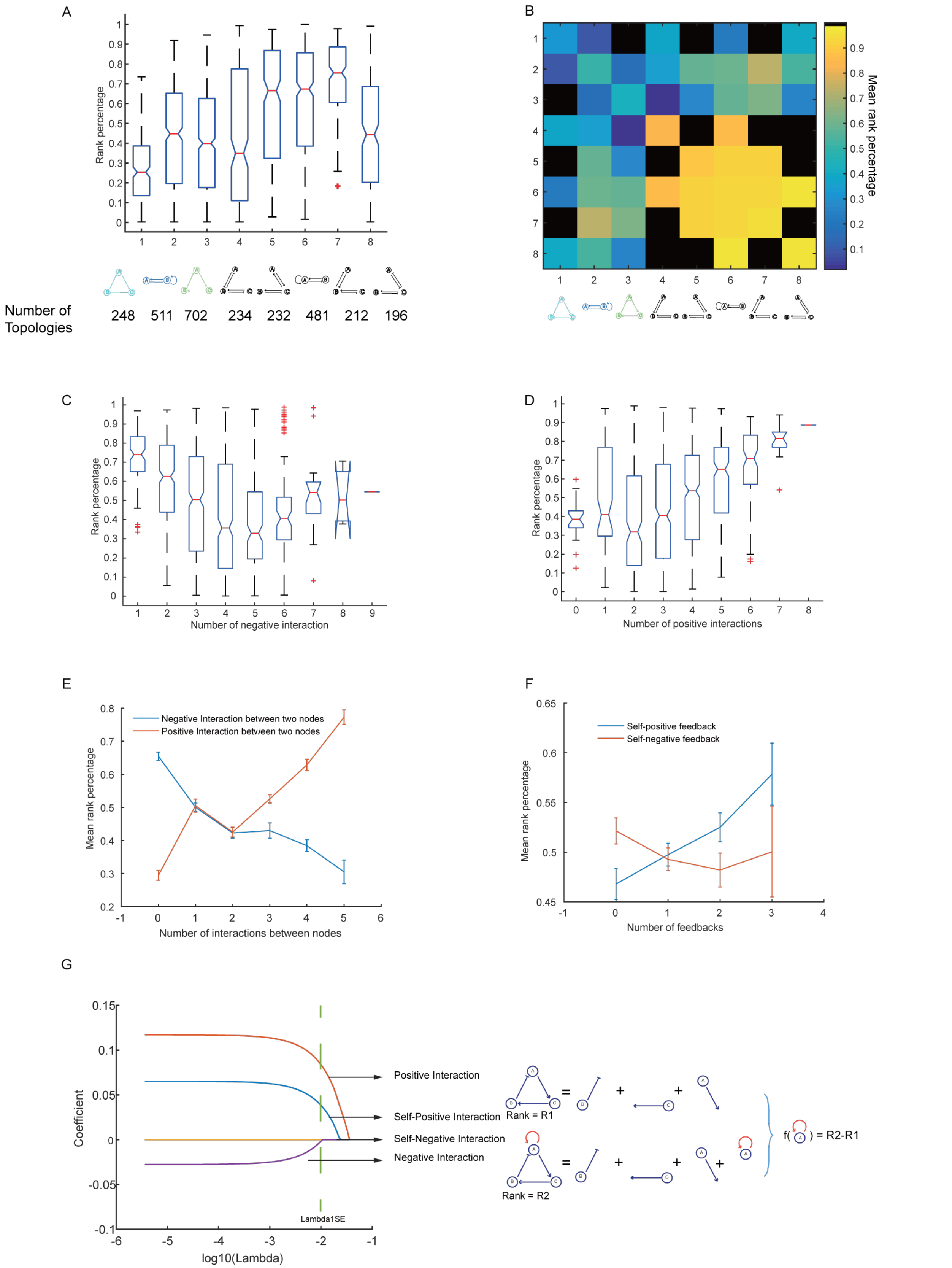

Figure S1. Relationship between oscillator topology and robustness. Related to Figure 1. (A) Distributions of the rank percentage of the Q value of topologies that contain certain oscillatory cores. Note that here, in contrast to Figure 1D, the topologies may contain more than one cores. (B) Effects from pairwise combinations between any two of the eight oscillatory cores. The heat map shows mean rank percentage of the Q value of topologies that only contain one (diagonal) or two oscillatory cores (off-diagonal). The black square indicates that no such topology exists. (C, D) Distributions of rank percentage of the Q value of topologies with various numbers of negative interactions (C) and positive interactions (D). (E) Effects of the node-to-node positive interaction and node-to-node negative interaction on robustness, showing that negative interaction may increase the robustness. (F) Effects of self-positive feedback and self-negative feedback on robustness, showing that self-negative feedback may decrease the robustness. (G) LASSO analysis on one edge modifications, showing that there are no significant one edge motifs that can increase the robustness without introducing new cores.

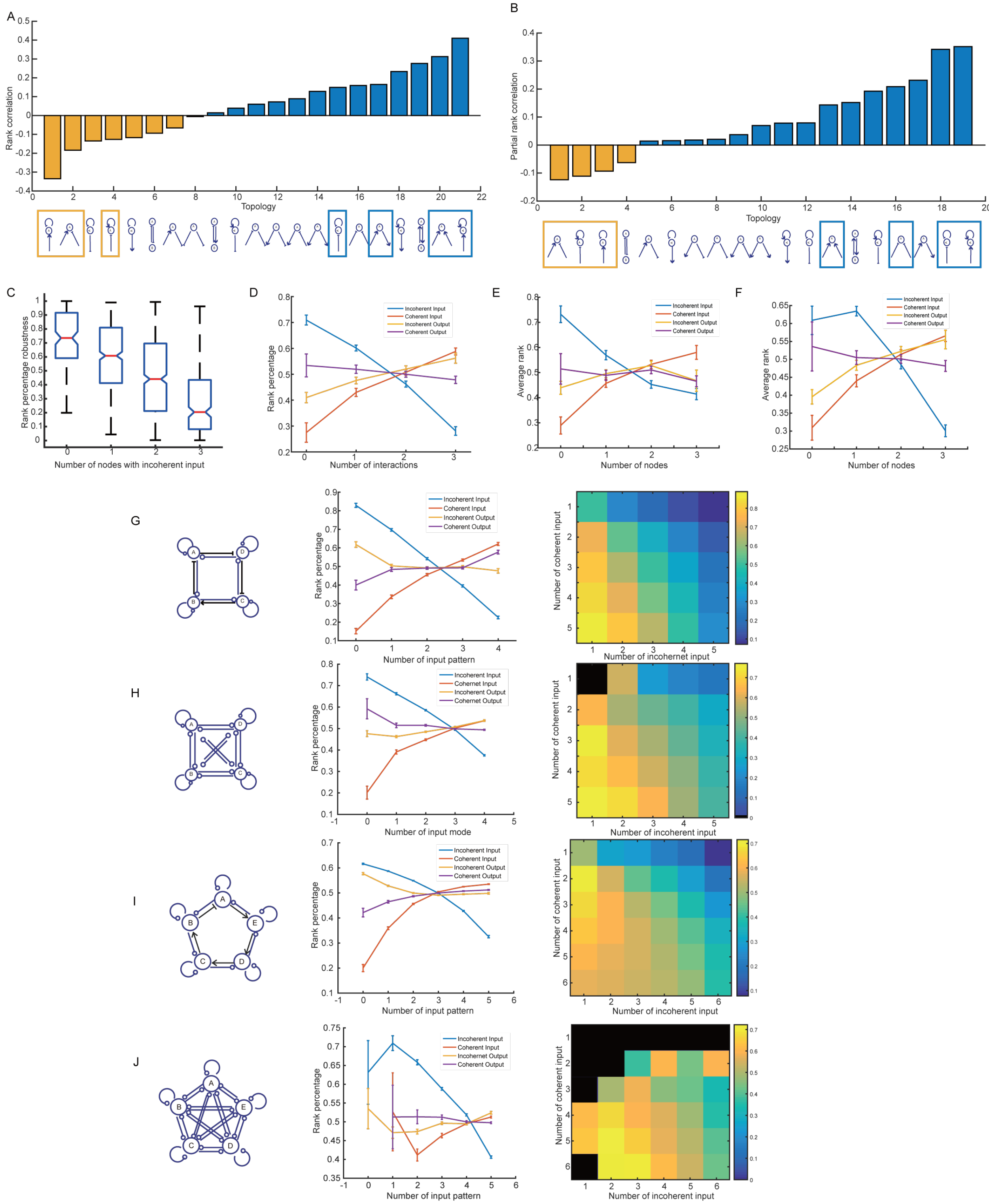
A
Rank correlation
Topology
B
Partial rank correlation
Topology
C
Rank percentage robustness
Number of nodes with incoherent input
D
Rank percentage
Number of interactions
Incoherent Input
Coherent Input
Incoherent Output
Coherent Output
E
Average rank
Number of nodes
F
Average rank
Number of nodes
G
Rank percentage
Number of input pattern
Number of coherent input
Number of incohernet input
H
Rank percentage
Number of input mode
Cohernet Input
Incoherent Output
Cohernet Output
Number of coherent input
Number of incoherent input
I
Rank percentage
Number of input pattern
Number of coherent input
Number of incoherent input
J
Rank percentage
Number of input pattern
Incohernet Output
Number of coherent input
Number of incoherent input

Figure S2. Incoherent inputs improve the robustness of biological oscillators in network enumeration. Related to Figure 2. (A) Spearman's rank correlation between the changes in the rank percentage of the Q value of a topology and a two-edge modification. B. Partial rank correlation between the change in the rank percentage of the Q value of a topology and a two-edge modification (controlling other two-edge modifications). Note that two motifs with the lowest rank correlation are dropped to avoid linear correlation of inputs. (C) Distribution of the rank percentage of the Q value of topologies with different number of incoherent inputs. (D-F) The relationship between the mean rank percentage of the Q values and the number of nodes with different input logic. The calculation is done using normal settings (D), linear sampling (E), a Michaelis-Menten type interaction function (F). (G-J) The left panels show network topologies (as in Figures 2E-H). The middle panels show the relationship between the mean rank percentage of the Q values and the number of nodes with different input logic. The right panels show the mean rank percentage of the Q values as a function of the number of coherent inputs and the number of incoherent inputs the topologies contain.

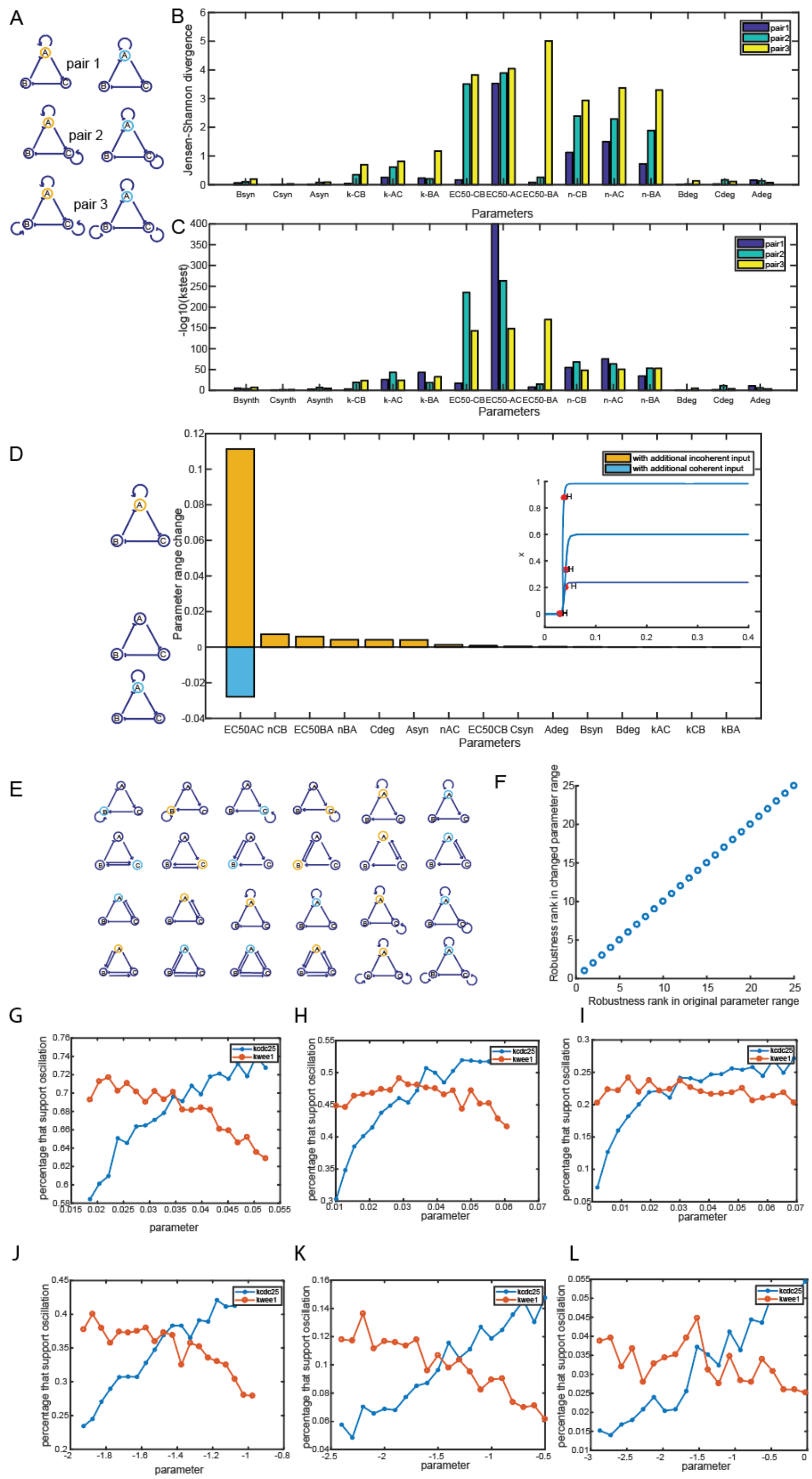
A
pair 1
pair 2
pair 3
B
Jensen-Shannon divergence
Parameters
C
-log10(kstest)
Parameters
D
Parameter range change
with additional incoherent input
with additional coherent input
EC50AC nCB EC50BA nBA Cdeg Asyn nAC EC50CB Csyn Adeg Bsyn Bdeg kAC kCB kBA
Parameters
E
F
Robustness rank in changed parameter range
Robustness rank in original parameter range
G
H
I
J
K
L
percentage that support oscillation
parameter
kcdc25
kwee1

Figure S3. Incoherent input increases the viable range of binding efficiency. The effect of incoherent input is consistent with different sampling parameter ranges. Related to Figure 2 and Figure 3. A, To identify which parameters are sensitive to incoherent inputs, three pairs of exemplary topologies were compared over each of the four types of parameters. There are four types of parameters in our model: 1. basal activation and inactivation rates. 2. k (enzymatic reaction rate constants). 3. K (thresholds of the activation or inactivation; K is equivalent to the half-maximal response concentration. 4. n (Hill coefficients of interactions). B. Jensen-Shannon divergence of single-parameter distributions between each pair of topology, showing that the distributions of K and Hill coefficient are changed the most. C. p-value of the two-sample Kolmogorov–Smirnov test, showing that the distribution of K is changed most significantly. D. Left: Bifurcation range difference (scaled by sampling range) between repressilator (middle topology) and the repressilator with a self-positive (top topology) or a self-negative (bottom topology) feedback. The parameter center is the centroid of parameters that support oscillations. Right: an example of bifurcation point on x-y null-clines, showing that larger nullcline range is associated with larger K range. E, Example topologies used to test the effect of parameter range choice. F, Ranks of Q values of topologies with original versus new ranges (10X upper range or 0.1X lower range). Note that all topologies remained the same ranks in all parameter range permutations. G~L, Percentage of parameters that support oscillations with the change of k_{cdc25} (incoherent input) and k_{wee1} (coherent input). G, linear sampling, 0~200% default value. H, linear sampling, 25~175% default value. I linear sampling 50~150% default value. J, log sampling, 0.32x~3.2x default value. K, log sampling, 0.1x~10x default value. L, log sampling, 0.032x~32x default value. All default values are based on published research (Tsai et al., 2014).

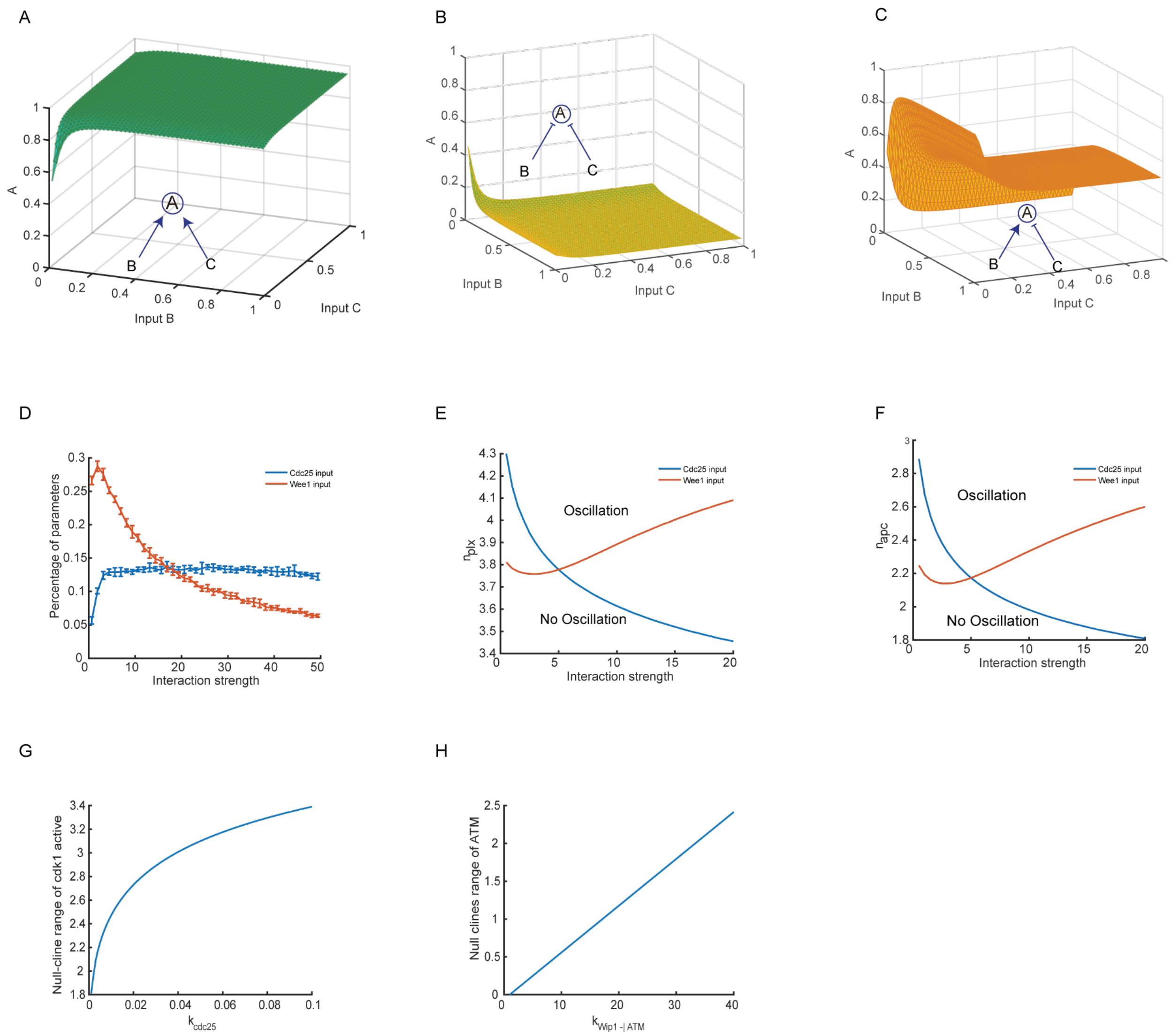

Figure S4. Incoherent inputs improve the robustness in real-world biological oscillator models. Related to Figure 3. (A-C) Null-planes of systems where a node receives coherent inputs (A, B) or incoherent inputs (C) from two different sources. Basal reaction rate = 0.1, self-regulation rate = 1, input rate = 10, EC50 = 0.1, n = 2. The results show that incoherent inputs can increase the range of a variable's steady states. (D) Percentage of parameters that yield sustained oscillations changes with increasing interaction strength of Cdc25 (p1) or Wee1 (p2). The parameter ranges of simulation are shown in Table S2. It shows that strong cdc25 can benefit robust oscillations. (E, F) Hopf bifurcation diagram of n_{plx} (E) and n_{apc} (F) with Cdc25 interaction strength and Wee1 interaction strength. (G) Nullcline range of active Cdk1 changes with increasing k_{cdc25}. (H) Nullcline range of ATM changes with $k_{wip1-|ATM}$.